

Aspects on Data Analysis and Visualization for Complex Dynamical Systems

J. Becker¹, D. Bürkle¹, R.-T. Happe¹, T. Preußner², M. Rumpf², M. Spielberg², and
R. Strzodka²

¹ Universität Freiburg

² Universität Bonn

Abstract. Flow visualization is an indispensable tool for the understanding of complex flow phenomena in computational fluid dynamics and the analysis of dynamical systems. In this note we will present several ways for an effective post processing of fluid flows and flows on invariant manifolds of dynamical systems. Feature extraction techniques will be present which reduce the informational content of large time-dependent data sets to its mainly interesting essence. Furthermore, we present visualization approaches which are based on partial differential equations. Similar to the modelling of physical phenomena by partial differential equations, in the postprocessing of data such equations naturally arise as well. Finally, the method for the dense covering of an invariant manifold with streamlines is outlined, which enables us to represent the geometry of the objects, statistical information on it, and the local flow properties at the same time.

1 Introduction

The understanding of complex structures in dynamical systems is a challenging subject not only from the analytical or numerical point of view. Visualization serves as a tool to get insight in solution structures and their dynamical behaviour. Frequently, standard methods for a graphical representation break down almost at the beginning. For instance the visualization of time-dependent vector fields by arrow icons leads to visual clutter, or drawing single orbits on invariant manifolds often hides important features of this object. Furthermore, for time-dependent problems especially in 3D, a drawing of complicated geometric pattern often hides essential information, e. g. in terms of critical points, heteroclinic and homoclinic orbits. We will describe recent approaches from different fields of dynamical systems to avoid these shortcomings. Therefore, we gather brief descriptions of several methods and algorithms in this note. Detailed discussions of these techniques can be found in publications, where they have been presented first [3,19,7,4,10,14,2]. Here, our main intention is to describe them as bricks of diverse origin but with the same aim to enable a better understanding of complex flow phenomena in computational fluid dynamics and the theory of dynamical systems. Our goal is to graphically represent flow data in an intuitively understandable and precise way.

At first, we will discuss feature extraction techniques for fluid flow. If we are interested in the topology of flow fields, we may focus on the evolution of critical points, connecting orbits, or vortex cores. Iconic visualization techniques will be presented,

which help to extract such features and to visualize them in an intuitively acceptable way.

Furthermore, two methods based on a modelling with partial differential equations are described which allow an easy perception of flow data. The texture transport method especially applies to time-dependent velocity fields. Lagrangian coordinates are computed solving the corresponding linear transport equations numerically. Choosing an appropriate texture on the reference frame the coordinate mapping can be used as a suitable texture mapping. Alternatively, the nonlinear diffusion method serves as an appropriate scale space method for the visualization of complicated flow patterns. It is closely related to nonlinear diffusion methods in image analysis where images are smoothed while still retaining and enhancing edges. Here an initial noisy image is smoothed along streamlines, whereas the image is sharpened in the orthogonal direction. The two methods have in common that they are based on a continuous model and discretized only in the final implementational step. Therefore, many important properties are naturally established already in the continuous model.

Concerning invariant manifolds of dynamical systems, a novel visualization approach is presented. It is based on research concerning efficient and robust set oriented computational methods, which were introduced by M. Dellnitz, T. Hohmann, and O. Junge [8,9]. Thereby the manifolds are covered with leaf boxes of a binary tree of boxes. The visualization technique to be presented here allow an interactive manipulation and inspection of these sets and an accompanying invariant measure density. Furthermore to struggle out the local dynamics, a covering of the leaf boxes with a dense set of short integral lines is considered. These line segments can then be shaded and animated.

To introduce the general topic, let us briefly recall the principle setting of flow visualization. The visualization of field data, especially of velocity fields from CFD computations is one of the fundamental tasks in scientific visualization. The simplest method to draw vector plots at nodes of some overlaid regular grid in general produces visual clutter, because of the typically different local scaling of the field in the spatial domain, which leads to disturbing multiple overlaps in certain regions, whereas in other areas small structures such as eddies can not be resolved adequately. The central goal is to obtain a denser, intuitively better acceptable method. Furthermore it should be closely related to the mathematical meaning of field data, which is mainly expressed in its one to one relation to the corresponding flow. Single particle lines only very partially enlighten features of a complex flow field. Thus, we ask for an *automatic selection procedure of interesting particle lines and features* or alternatively a *suitable dense pattern which represents the flow ϕ globally on the computational domain*.

2 Iconic Visualization of Flow Phenomena

Complex physical phenomena can be simulated and resolved with large scale computations based on recent numerical methods, in particular adaptive, time-dependent,

two and three dimensional finite element or finite volume algorithms based on unstructured grids. Characteristics of the solution, which are topologically invariant and globally describe the physical phenomena, are in general hidden in enormous masses of information. Instead of an “overall” visualization, concepts to display selected important aspects are required. We are forced to carefully depict these features of interest, which characterize the global solution. A couple of selection techniques has recently been studied. Globus et al. [13] propose to extract critical points from flow data sets. At these locations they graphically represent the eigenspaces. On boundary shapes, Helman and Hesselink [15] construct topological skeletons for vector fields. In [11] Demarcelle and Hesselink give a complete analysis of second order tensor field topology on two dimensional domains. Post et al. [18] apply methods based on mathematical morphology to locate interesting regions in large data sets. To represent the local solution in regions of interest graphically, icons have been investigated. An icon is a geometric object which acts as a symbolic representation for specific data quantities and features of the solution. DeLeeuw and van Wijk [16] have developed an iconic flow probe. Post et. al. [18] give several glyphs for various simulation features.

In this section we contribute new icons and criteria for point selection and apply them in different stationary and especially time-dependent applications.

At first let us consider the linearization of a flow close to a particle path. We pick up the above one-to-one relation between a velocity field and the induced flow φ defined by the ordinary differential equation

$$\dot{\varphi}(X, t) = v(\varphi(X, t), t)$$

where $\varphi(X, 0) = X$ describes the motion of particles initially located at positions X driven by the velocity v in Eulerian coordinates. Therefore the above equation can be rewritten as $\dot{x} = v(x, t)$. Now we ask for the acceleration \ddot{x} of a particle. By applying the chain rule we obtain the material derivative Dv/dt ($Dv/dt = \partial_t v + v \cdot \nabla v$ by definition) of the velocity v :

$$\ddot{x} = \frac{\partial}{\partial t} v + v \cdot \nabla v = \frac{D}{dt} v$$

If this derivative vanishes on a particle path, the corresponding particle is up to first order in a constant motion. Now let us assume we have selected some particle of interest denoted x_0 at time t_0 . Its path can be expanded in terms of v and $\frac{D}{dt} v$

$$x_0(t) = x_0(t_0) + v(x_0, t_0)(t - t_0) + \frac{1}{2} \frac{D}{dt} v(x_0, t_0)(t - t_0)^2 + O\left(\frac{\partial^3}{\partial t^3}\right)$$

We will study the motion of nearby particles moving along the latter path more closely and expand the offset

$$(x - x_0)(t) = (x - x_0)(t_0) + (v(x, t_0) - v(x_0, t_0))(t - t_0) + \frac{1}{2} \left(\frac{D}{dt} v(x, t_0) - \frac{D}{dt} v(x_0, t_0) \right) (t - t_0)^2 + O((t - t_0)^3)$$

$$= (x - x_0)(t_0) + \nabla v(x_0, t_0)(t - t_0)(x - x_0) + \frac{1}{2} \nabla \frac{D}{dt} v(x_0, t_0)(t - t_0)^2(x - x_0) + O((t - t_0)^3 + (t - t_0)(x - x_0)^2)$$

Linearizing this equation we obtain

$$\dot{\delta} = \nabla v(x_0, t_0)\delta \quad \delta(0) = \delta_0$$

To summarize, the first order motion in a neighbourhood of a specific particle x_0 at time t_0 is described by the velocity $v(x_0, t_0)$ and the velocity gradient $\nabla v(x_0, t_0)$. Now we ask for a graphical representation of this offset motion. Therefore let us look closer onto the induced linear field. We will restrict ourselves to the three dimensional case. The considerations in two dimensions then are a straightforward consequence. ∇v has at least one real eigenvalue, which we will suppose to be the third. The others might be real as well or conjugate complex. If the real parts of all three eigenvalues are positive, respectively negative, x is a moving source respectively sink. The flow of an incompressible medium in a closed system is source and sink free. To facilitate the exposition, let us restrict to this case. For differentiable velocities incompressibility is equivalent to vanishing divergence. By that assumption in the nondegenerate case there is a two dimensional subspace of \mathbb{R}^3 spanned by the eigenvectors corresponding to the eigenvalues of equal sign (resp. to the complex eigenvalue and its conjugate) and one remaining direction corresponding to the third eigenvalue. The induced flow is hyperbolic, particles stream in along the plane and they stream out of x in the direction of the third eigenvector, or vice versa. Graphically the direction of the third eigenvalue is represented by two opposite vectors positioned at x and pointing in or out, depending on the sign of the corresponding eigenvalue. If the other two eigenvalues of opposite sign are real, we display the restricted sink or source type flow by a disk centered at x , scale the two eigenvectors by the eigenvalues and place them on the disk. In the complex conjugate case the restricted flow is swirling in or out on the plane. To support an intuitive understanding we partition the above disk into 4 segments with alternating colour. The real part of the eigenvalue $\lambda = \alpha + i\beta$ drives the particles into the center or away from it proportionally to $e^{\alpha t}$. That determines the period of time τ the particles need to traverse the disk. Afterwards, they'll have been swirled around the angle $\beta\tau$. The rim of the disk is twisted according to that angle, and the disk is deformed linearly as indicated by the real and imaginary parts of the complex eigenvector. This leads to spiral shaped segments. The separation lines between the segments can be interpreted as first order relative particle paths.

Icons can be released at positions related to the domain geometry and yield first insights in solution aspects. Fig. 1 depicts an example, where the incompressible Navier–Stokes equations are solved in a rectangular box with walls inside, one outlet and one inlet model the flow in a water reservoir. Some particle traces in the stationary flow field indicate the principal motion. The three–dimensional structure of the recirculation zones is visualized by placing columns of icons in the volume. Each icon shows the rotation of the velocity evaluated at its center. Especially for flow problems icons can be aligned to particle lines [16]. But one has to be very careful

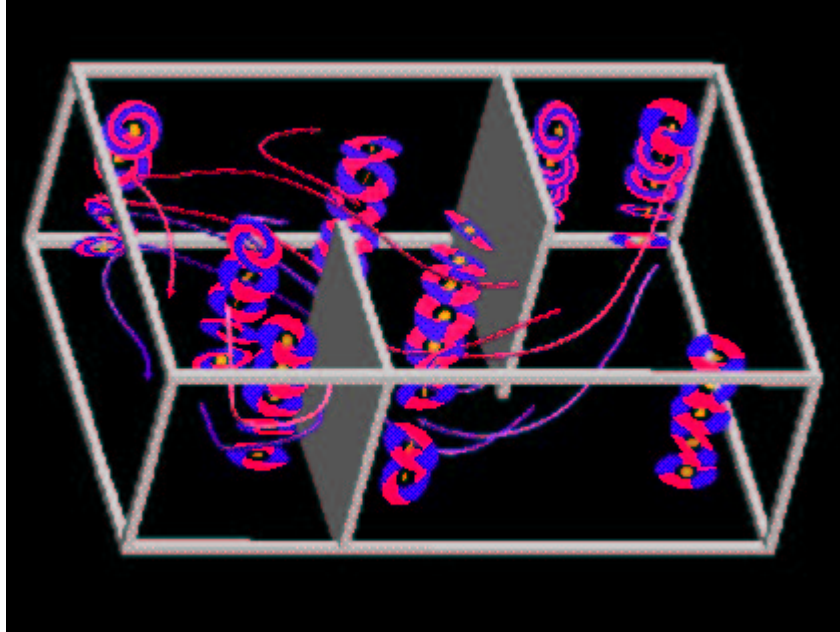


Fig. 1. Rotation icons in an incompressible flow.

in finding appropriate paths which give significant insight in interesting qualitative aspects of the underlying phenomena. Critical points, characterized by $v = 0$, are of specific interest in velocity fields, in particular in the stationary case. They are topological invariants of the underlying flow [1] and can be taken as seed points to reconstruct a topological skeleton. Fig. 2 shows icons visualizing the local flow at critical points extracted automatically from a three dimensional volume. The underlying interpretation has already been discussed above. In the non stationary case critical points do not have the same meaning as for stationary velocity fields. But nevertheless they are still topologically invariant and give insight in qualitative aspects of the flow. Fig. 3 shows several snapshots of the incompressible, nonstationary flow behind an obstacle in two dimensions. It enlightens part of the process responsible for the formation of a Karman vortex street. Finally, Fig. 4 shows icons and streamlines on the homoclinic, respectively heteroclinic orbits in a convective flow.

3 Vector Field Aligned Nonlinear Diffusion

Let us now discuss a first PDE based method. Here, nonlinear anisotropic diffusion applied to some initial random noisy image will enable an intuitive and scalable visualization of complicated flow fields. Therefore, we pick up the idea of line integral convolution, where a strong correlation in the image intensity along streamlines is

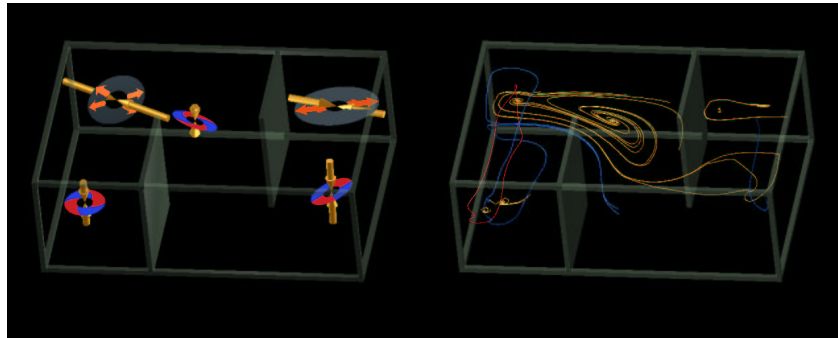


Fig. 2. On the left icons placed at critical points in an incompressible flow in three dimensions, on the right the critical points are taken as starting point for particle lines.

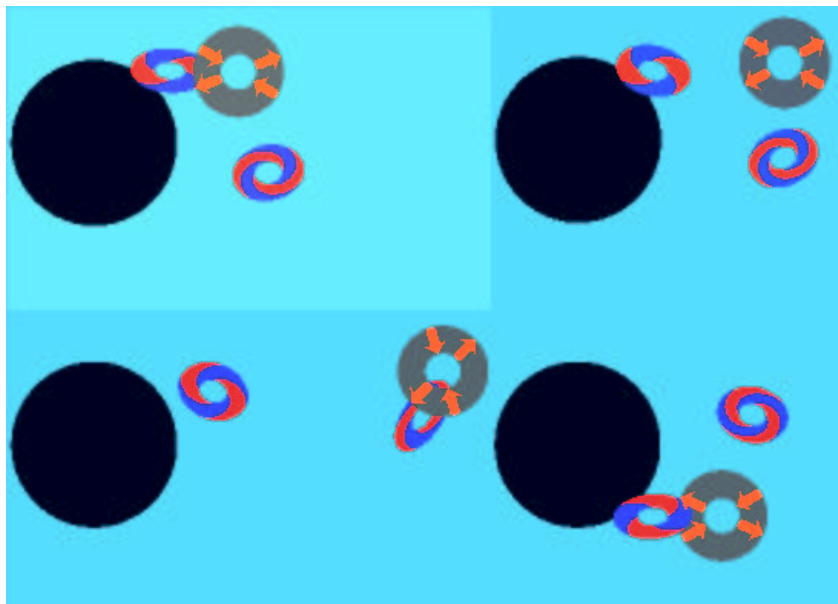


Fig. 3. Icons placed at critical points in a non stationary, incompressible flow

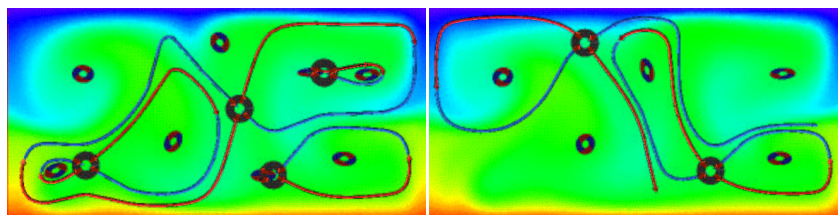


Fig. 4. The topology of a convective flow in 2D depicted by icons and selected streamlines for two timesteps.

achieved by convolution of an initial white noise along the streamlines. As proposed already by Cabral and Leedom [5,21] a suitable choice for the convolution kernel is a Gaussian kernel. On the other hand an appropriately scaled Gaussian kernel is known to be the fundamental solution of the heat equation. Thus, line integral convolution is nothing else than solving the heat equation in 1D on a streamline parametrized with respect to arclength. If we ask for a wellposed *continuous* diffusion problem with similar properties, we are lead to some anisotropic diffusion, now controlled by a suitable diffusion matrix. In the direction perpendicular to the flow field we incorporate a sharpening process known from scale space methods in image processing [17]. In detail we consider the following parabolic differential equation problem:

$$\begin{aligned} \frac{\partial}{\partial t} \rho - \operatorname{div} (A(\nabla \rho_\epsilon) \nabla \rho) &= f(\rho), & \text{in } \mathbb{R}^+ \times \Omega, \\ \rho(0, \cdot) &= \rho_0, & \text{on } \Omega, \\ \frac{\partial}{\partial \nu} \rho &= 0, & \text{on } \mathbb{R}^+ \times \partial \Omega \end{aligned}$$

for given initial density $\rho_0 : \Omega \rightarrow [0, 1]$. Here $\rho_\epsilon = \chi_\epsilon * \rho$ is a mollification of the current density. This ensures the wellposedness of the above parabolic, boundary and initial value problem. In our setting we interpret the density as an image intensity, a scalar greyscale or – with a slight extension to the vector valued case – as a vector valued color. Thus, the solution $\rho(\cdot)$ can be regarded as a family of images $\{\rho(t)\}_{t \in \mathbb{R}^+}$, where the time t serves as a scaling parameter.

Let us now focus on the anisotropic diffusion matrix A . For a given vector field $v : \Omega \rightarrow \mathbb{R}^n$ we consider linear diffusion in the direction of the vector field and a Perona Malik type diffusion orthogonal to the field. If we suppose that v is continuous and $v \neq 0$ on Ω , then there exists an family of continuous orthogonal mappings $B(v) : \Omega \rightarrow SO(n)$ such that $B(v)v = e_0$, where $\{e_i\}_{i=0, \dots, n-1}$ is the standard base in \mathbb{R}^n . Thus we define

$$A(v, d) = B(v)^T \begin{pmatrix} \alpha(\|v\|) & \\ & G(d) \operatorname{Id}_{n-1} \end{pmatrix} B(v)$$

where $\alpha : \mathbb{R}^+ \rightarrow \mathbb{R}^+$ is a supposed to be monoton, controlling the linear diffusion in vector field direction, i. e. along streamlines, and $G(\cdot)$ acts as an edge enhancing diffusion coefficient in the orthogonal directions (cf. [23,17]), e. g. $G(d) = \beta (1 + \|d\|^2)^{-1}$. As initial data ρ_0 we choose some random noise of an appropriate frequency range.

Hence pattern will grow upstream and downstream, whereas the edges tangential to these patterns are successively enhanced. Still there is some diffusion perpendicular to the field which supplies us for evolving time with a scale of progressively coarser representation of the flow field. If we run the evolution for vanishing right hand side f the image contrast will unfortunately decrease due to the diffusion along streamlines. Therefore, we strengthen the image contrast during the evolution, selecting an appropriate function $f : [0, 1] \rightarrow \mathbb{R}^+$, with $f(0) = f(1) = 0$, $f > 0$ on $(0.5, 1)$, and $f < 0$ on $(0, 0.5)$.

If we ask for pointwise asymptotic limits of the evolution, we expect an almost everywhere convergence to $\rho(\infty, \cdot) \in \{0, 1\}$ due to the choice of the contrast en-

hancing function $f(\cdot)$ (cf. Fig. 5). The space of asymptotic limits significantly

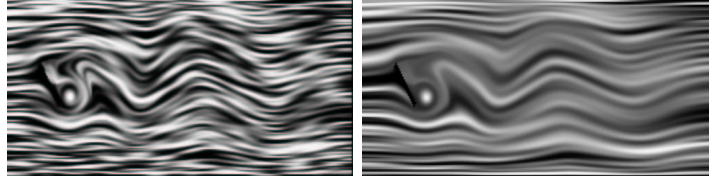


Fig. 5. A single timestep is depicted from the nonlinear diffusion method applied to the vector field describing the flow around an obstacle at a fixed time. A discrete white noise is considered as initial data. We run the evolution on the left for a small and on the right for a large constant diffusion coefficient α .

influences the richness of the developing vector field aligned structures. To enrich the set of asymptotic states settled by anisotropic diffusion we can consider a vector valued $\rho : \Omega \rightarrow [0, 1]^m$ for some $m \geq 1$ and a corresponding system of parabolic equations. Finally we end up with the method of nonlinear anisotropic diffusion to visualize complex vector fields [20] (cf. Fig. 6).

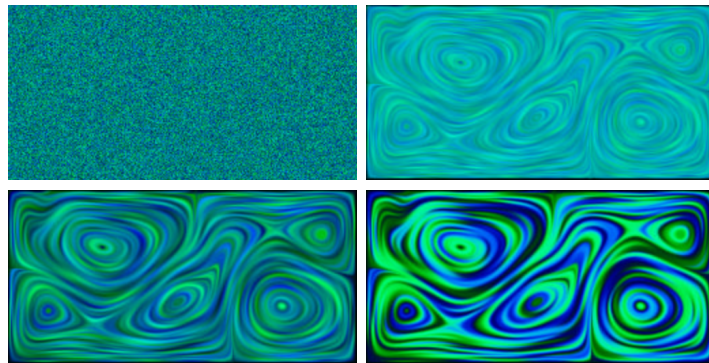


Fig. 6. Several diffusion timesteps are depicted from the vector valued nonlinear anisotropic diffusion method applied to a convective flow field in a 2D box.

4 Texturing Lagrangian Coordinates

The second method based on a modelling with partial differential equations consists in the numerical calculation of the flux ϕ itself [3]. We adopt the idea of the implicit streamsurfaces presented by J. van Wijk [24] and discuss the corresponding transport problem for time-dependent data. Inflow time and inflow coordinates

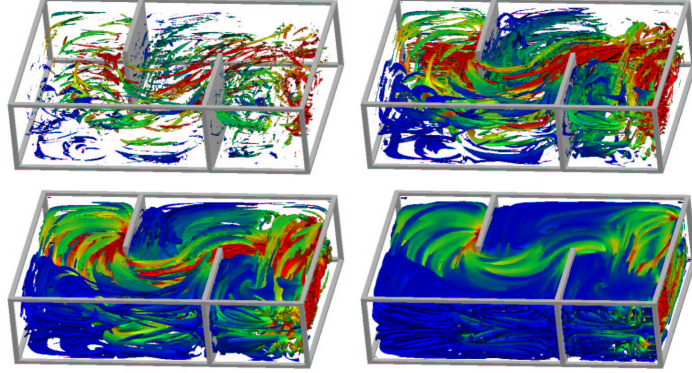


Fig. 7. The incompressible flow in a water basin with two interior walls and an inlet (on the left) and an outlet (on the right) is visualized by anisotropic nonlinear diffusion. Color is indicating the velocity.

may be regarded as a Lagrangian frame. The method we propose here displays Lagrangian coordinates by texture mapping, which map a certain pattern from a Lagrangian coordinates system, i. e. from texture space, to the Eulerian frame. Let us assume $\Omega \subset \mathbb{R}^n$ to be a domain describing a fluid container with an inlet boundary $\Gamma^+ \subset \partial\Omega$ and an outlet boundary $\Gamma^- \subset \partial\Omega$. Furthermore we suppose the fluid velocity $v : \Omega \times [0, \hat{T}] \rightarrow \mathbb{R}^n$ to be given for a fixed time \hat{T} . In the application this velocity will be delivered by a numerical simulation, which runs simultaneously or has stored its results in files on disk. Let us now interpret the coordinates X on the inlet boundary Γ^+ , respectively the inflow time T as depending variables, which are transported with the fluid. Then they are described by the following transport equation for a density ρ

$$\begin{aligned} \partial_t \rho + v \cdot \nabla \rho &= 0 & \text{in } \Omega, \\ \rho &= \rho_\Gamma & \text{on } \Gamma^+. \end{aligned}$$

Thus we obtain $\rho = X$ for $\rho_\Gamma = X$ on Γ^+ , respectively $\rho = T$ for $\rho_\Gamma = T$ on Γ^+ . On the outlet Γ^- no boundary condition has to be described if $v \cdot \nu \geq 0$ for all times, where ν is the outer normal of the domain Ω . This transport can be interpreted as a simultaneous and global particle tracing. On a particle path $x(t)$ the solution ρ of the above transport equation is constant, because $\dot{x}(t) = v(x(t), t)$ and

$$\begin{aligned} \frac{d}{dt} \rho(x(t), t) &= \partial_t \rho(x(t), t) + \dot{x}(t) \cdot \nabla \rho(x(t), t) \\ &= 0. \end{aligned}$$

Therefore points of constant X value are located on the particle line starting at position X on Γ^+ . Analogously a constant T value indicates points on a surface which is the image of a corresponding surface on the inlet under the flow $\phi(\cdot, T)$. In this

sense X, T as functions on $\Omega \times [0, \hat{T}]$ can be regarded as Lagrangian coordinates describing the motion of particles which pass through Γ^+ . Particles which have earlier entered the fluid container are not considered so far.

The transport equation becomes a wellposed problem by prescribing suitable initial conditions. If every particle path starting at a position in Ω has left the domain, the solution ρ no longer depends on these initial conditions. For moderate values of \hat{T} this might not be the case and for certain applications especially the initial phase of the physical simulation is of great importance. Therefore we suppose that \tilde{X} and \tilde{T} are extensions of $X|_{\Gamma^+}$ respectively 0 on Ω and choose them as initial conditions for the two transport problems. E. g. if $\Omega \subset \mathbb{R}^+ \times \mathbb{R}$ and $\Gamma_+ \subset 0 \times \mathbb{R}$ we choose $\tilde{X}(x_1, x_2) = (0, x_1)$, $\tilde{T}(x_1, x_2) = 0$.

Finally, we have to define an appropriate pattern in the texture space $\Gamma^+ \times [0, \hat{T}]$. There are several desirable features which should be realized by the textural representation of the Lagrangian coordinates. It should simultaneously code time and inlet coordinates. Furthermore, to enable long time animation of moving fluids the pattern in the texture space should be periodic in T and the zooming into detailed areas has to be supported by a scalability property. Thus, we use a periodic color coding of T and a periodic scalable 1D texture for X (cf. Fig. 8, 9).

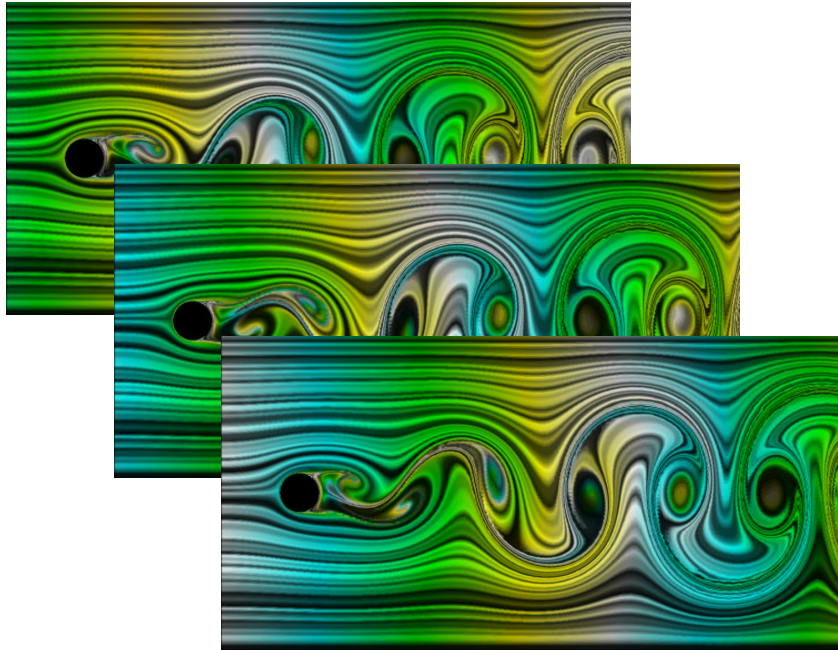


Fig. 8. Texture transport in the von Kármán vortex street.

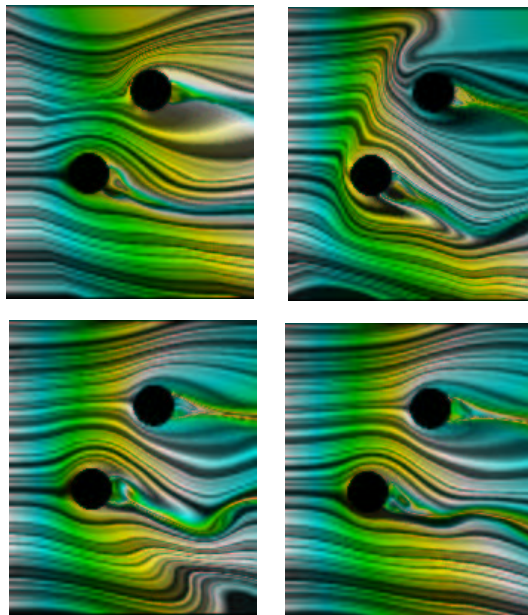


Fig. 9. Texture transport applied to a compressible Euler flow around two obstacles.

5 Streamlines on Invariant Manifolds of Dynamical Systems

In this final section we will deal with a dense coverage of approximations of invariant manifolds with streamlines. They display the local flow on the manifold in an intuitively understandable way. This method is an analog of the techniques presented before, but now on geometrically complex objects. To begin with, let us consider a dynamic system. If time is assumed to evolve continuously then this system is frequently given by an ordinary differential equation of the form

$$\frac{dx}{dt}(t) = g(x), \quad (1)$$

where $g : \mathbb{R}^n \rightarrow \mathbb{R}^n$. Alternatively, we may study a discrete dynamical system of the form

$$x_{j+1} = f(x_j), \quad j = 0, 1, \dots, \quad (2)$$

where $f : \mathbb{R}^n \rightarrow \mathbb{R}^n$. Observe that this type of dynamical system naturally arises when an ordinary differential equation is integrated by an explicit numerical scheme. Topological information on the long term behavior of the dynamical system is given by invariant sets: a set $A \subset \mathbb{R}^n$ is *invariant* if

$$f(A) = A.$$

In this section we present a visualization techniques based on recent numerical approximation methods by D. Dellnitz, H. Hohmann, O. Junge. The central object

which is approximated by the subdivision algorithm developed in [9] is the so-called *relative global attractor*,

$$A_Q = \bigcap_{j \geq 0} f^j(Q), \quad (3)$$

where $Q \subset \mathbb{R}^n$ is a compact subset. Roughly speaking, the set A_Q should be viewed as the union of invariant sets inside Q together with their unstable manifolds. In particular, A_Q may contain subsets of Q which cannot be approximated by direct simulation. A subdivision algorithm for the approximation A_Q^k of A_Q generates a sequence $\mathcal{B}_0, \mathcal{B}_1, \dots, \mathcal{B}_k, \dots$ of finite collections of boxes which contain A_Q and approximate this relative invariant set for increasing values of k . In the concrete implementation the boxes are generalized rectangles which build up a binary tree, generated by successive bisection [8]. As an example we study here invariant set in the Lorenz system [7]. Once a box covering \mathcal{B} of the attractor A_Q has been computed, one can approximate the statistics of the dynamics on A_Q by the computation of a corresponding natural invariant measure. I. e. the transition probabilities

$$p_{ij} = \frac{m(f^{-1}(B_i) \cap B_j)}{m(B_j)}, \quad i, j = 1, \dots, N$$

can be approximated, where m denotes Lebesgue measure. Then an eigenvector for the eigenvalue 1 is computed numerically and serves as an approximation of the invariant measure. We will use this measure for coloring of the flow lines.

The set oriented algorithm is not restricted to approximations of attracting sets which are smooth submanifolds of \mathbb{R}^n . The attractor under consideration may have a Hausdorff dimension which is not an integer but is of dimension between two and three. Nevertheless, frequently attractors are contained in the closure of unstable manifolds which are locally m dimensional surfaces within \mathbb{R}^n . Unfortunately, this surface structure is hidden in our discrete box approach. In terms of a surface interpretation the fundamental question is how to define a tangent space, or, equivalently, how to give a suitable definition of normals. Here we apply a method related to Nielson's approach in the interpolation of scattered data [6]. For given ϵ we consider the neighbourhood $U_\epsilon(c_B)$ of the center point c_B of every box $B \in \mathcal{B}_k$. (The distance is measured in the maximum norm.) Then we define the local center of gravity \bar{x}_B and the first momentum matrix S_B by

$$\bar{x}_B = \int_{U_\epsilon(c_B) \cap A_Q^k} dx, \quad S_B = \frac{3}{\epsilon^2} \int_{U_\epsilon(c_B) \cap A_Q^k} (x - \bar{x}_B)(x - \bar{x}_B)^T dx.$$

The scaling of S_B obviously guarantees that $S_B = Id$, if the invariant set completely covers $U_\epsilon(c_B)$. Concerning the implementation we can avoid the exact evaluation of the integrals and approximate them by a counting measure over box centers. We thereby take into account values of ϵ which are multiples of the length of box edges, e. g. in the applications we consider a factor of 10.

The momentum matrix S_B is symmetric. Thus, there exists an orthonormal system of eigenvectors v_1, \dots, v_n and corresponding real eigenvalues $\lambda_1 \leq \lambda_2 \leq \dots \leq$

λ_n . By construction the approximate set A_Q^k is locally more extended in directions of eigenvectors with relatively large eigenvalues λ_j and vice versa. If the actual invariant set A_Q is locally an m dimensional surface, then it is reasonable to assume that A_Q^k reflects this property in the sense that there are $(n - m)$ small eigenvalues, i. e.

$$\lambda_1 \leq \dots \leq \lambda_{n-m} \ll \lambda_{n-m+1} \leq \dots \leq \lambda_n.$$

We make use of this fact and require in the algorithm that $\frac{\lambda_{n-m}}{\lambda_{n-m+1}} < \delta$ for a small constant δ , in our case 0.1. Then the eigenvectors v_1, \dots, v_{n-m} are interpreted as approximate normals and v_{n-m+1}, \dots, v_n as approximate tangent vectors. Concerning the visualization, in particular for $n = 3$ and $m = 2$ the definition of a normal allows an appropriate shading and thereby supports the visual reception of the streamline coverage of a complicated invariant manifolds.

Our streamline visualization approach is related to the method of illuminated streamlines introduced by Stalling et al. [22]. Here, a coverage of the frequently lower dimensional invariant manifolds is attained similar to the line art illustration method by Elber [12].

We use streamlines to emphasize the local dynamics on the invariant set A_Q , i. e. the direction and velocity of the continuous flow according to the underlying ODE. Streamlines are suitable tools to visualize such information. We will now describe an algorithm which generates a coverage of A_Q^k with streamlines at a prescribed density in a preprocessing step. Then, for the later on interactive rendering we use transparent illuminated streamlines and color them according to the invariant measure. For our case we make use of the approximate surface normals and therefore shade the individual streamlines with respect to these normals. We thus ensure the graphical representation of the *global geometry* and the *local dynamics* of the dynamical system at the same time while still retaining the *surface type appearance*.

Our coverage will be of equal density all over A_Q^k in the sense that the ratio $\gamma(B) := L(B)/m(B)$ of the sum $L(B)$ of the length of streamline segments in the boxes B of the binary tree and the local volume $m(B)$ is balanced. We achieve this by an iterative insertion process of streamlines of fixed length 2δ . We successively select starting positions x_0 , compute streamline segments $x : [-\delta, \delta] \rightarrow \mathbb{R}^n$ as numerical solutions of the ODE problems

$$\dot{x} = g(x); \quad x(0) = x_0$$

and distribute the local segments onto the corresponding boxes. Simultaneously we update the current densities $\gamma(B)$ on the involved boxes.

Fig. 10 shows results for the Lorenz system..

Acknowledgement

The authors would like to thank M. Dellnitz and O. Junge for the ongoing cooperation and exchange of ideas and to acknowledge Karol Mikula, Jarke van Wijk for inspiring discussions and many useful comments on flow visualization and image

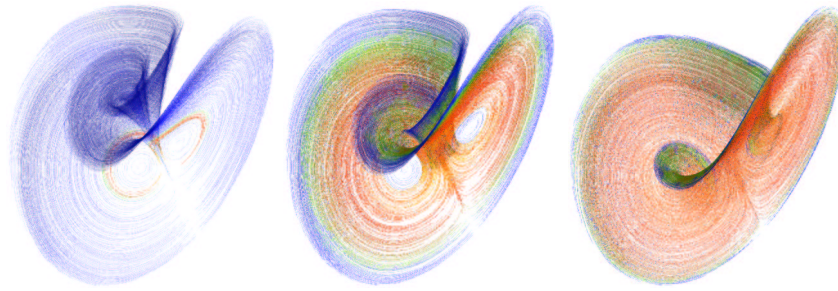


Fig. 10. Invariant sets in the Lorenz family are visualized using a coverage with shaded streamlines.

processing. Furthermore they thank Eberhard Bänsch from Bremen University for providing the incompressible flow data sets.

References

1. D. Asimov: Notes on the topology of vector fields and flows, Tutorial Notes, IEEE Visualization '95, 1995
2. J. Becker, T. Preußer, M. Rumpf: PDE Methods in Flow Simulation Post Processing, Computing and Visualization in Science, to appear
3. J. Becker, M. Rumpf: Visualization of time-dependent velocity fields by Texture Transport, Proceedings of the Eurographics Workshop on Scientific Visualization '98, Blaubeuren, 1998
4. D. Bürkle, M. Dellnitz, O. Junge, M. Rumpf, M. Spielberg: Visualizing Complicated Dynamics, Late Braking Hot Topics, Visualization '99
5. B. Cabral and L. Leedom. Imaging vector fields using line integral convolution. In J. T. Kajiya, editor, Computer Graphics (SIGGRAPH '93 Proceedings), volume 27, pages 263–272, Aug. 1993.
6. W. L. F. Degen and V. Milbrandt. The geometric meaning of nielson's affine invariant norm. CAGD, 15:19–25, 1997.
7. M. Dellnitz, A. Hohmann, O. Junge, and M. Rumpf. Exploring invariant sets and invariant measures. CHAOS: An Interdisciplinary Journal of Nonlinear Science, 7(2):221, 1997.
8. M. Dellnitz and A. Hohmann. The computation of unstable manifolds using subdivision and continuation, in Nonlinear Dynamical Systems and Chaos (H.W. Broer, S.A. van Gils, I. Hoveijn und F. Takens eds.), PNLDE 19 (Birkhäuser, 1996), 449-459.
9. M. Dellnitz and A. Hohmann, A subdivision algorithm for the computation of unstable manifolds and global attractors. Numerische Mathematik 75, 293-317, 1997.
10. M. Dellnitz, O. Junge, M. Rumpf, R. Strzodka: The computation of an unstable invariante set inside a cylinder containing a knotted flow, Proceedings of the EquaDiff '99
11. T. Delmarcelle, L. Hesselink: The Topology of Symmetric, Second-Order Tensor Fields, IEEE Visualization '94, 140–147, 1994
12. G. Elber. Line Art Illustrations of Parametric and Implicit Forms. IEEE Transactions on Visualization and Computer Graphics, 4 (1):71–81, 1998.
13. A. Globus, C. Levit, T. Lasinski: A Tool for Visualizing the Topology of Three-Dimensional Vector Fields, IEEE Visualization '91, 33–40, 1991

14. R.-T. Happe, M. Rumpf: Characterizing global features of simulation data by selected local icons, M. Gbel, J. David, P. Slavik, J.J. van Wijk (eds.): *Virtual Environments and Scientific Visualization'96*, Springer, Vienna 1996
15. J.L. Helman, L. Hesselink: Visualizing Vector Field Topology in Fluid Flows, *IEEE CG&A* 11, No. 3, 36–46, May 1991
16. W.C. Leeuw, J.J. van Wijk: A Probe for Local Flow Field Visualization, *IEEE Visualization '93*, 39–45, 1993
17. J. Malik, P. Perona: Scale space and edge detection using anisotropic diffusion, *IEEE Computer Society Workshop on Computer Vision*, 1987
18. F.J. Post, T. van Walsum, F.H. Post, D. Silver: Iconic Techniques for Feature Visualization, *IEEE Visualization '95*, 288–295, 1995
19. U. Diewald, T. Preußer, M. Rumpf: Anisotropic Nonlinear Diffusion in Vector Field Visualization on Euclidean Domains and Surfaces, *Tans. Vis. and Comp. Graphics* 2000, to appear
20. T. Preußer, M. Rumpf: An Adaptive Finite Element Method for Large Scale Image Processing, *Journal of Visual Comm. and Image Repres.*, 11:183–195, 2000
21. D. Stalling, C. Hege: Fast and Resolution Independent Line Integral Convolution, *Proceedings SIGGRAPH '95*, 1995
22. D. Stalling, M. Zöckler, and H.-C. Hege. Fast display of illuminated field lines. *IEEE Transactions on Visualization and Computer Graphics*, 3(2), Apr.–June 1997. ISSN 1077-2626.
23. J. Weickert: *Anisotropic diffusion in image processing*, Teubner, Stuttgart 1998
24. J. J. van Wijk. Flow visualization with surface particles. *IEEE Computer Graphics and Applications*, 13(4):18–24, July 1993.